



Photoluminescence and time-resolved luminescence spectroscopy of novel $\text{NaBa}_4(\text{BO}_3)_3:\text{Tb}^{3+}$ phosphor

Xinmin Zhang^{a,*}, Zhi Zhang^a, Hyo Jin Seo^{b,**}

^a School of Materials Science and Engineering, Central South University of Forestry and Technology, Changsha 410004, China

^b Department of Physics, Pukyong National University, 599-1, Daeyeon 3-Dong, Nam-Gu, Busan 608-737, Republic of Korea

ARTICLE INFO

Article history:

Received 29 November 2010

Received in revised form 26 January 2011

Accepted 27 January 2011

Available online 22 February 2011

Keywords:

Phosphors

Solid state reactions

Optical properties

Luminescence

Time-resolved optical spectroscopies

ABSTRACT

This paper reports the photoluminescence (PL) properties of Tb^{3+} in $\text{NaBa}_4(\text{BO}_3)_3$, as well as the time-resolved luminescence properties. The PL excitation spectrum exhibits intense $f \rightarrow f$ transition absorption; the PL emission spectrum shows the strongest ${}^5\text{D}_4 \rightarrow {}^7\text{F}_5$ emission at 540 nm. The relative intensity of ${}^5\text{D}_3$ emission is much weaker than that of ${}^5\text{D}_4$ emission even in the samples with lower Tb^{3+} concentration. The ${}^5\text{D}_3 \rightarrow {}^5\text{D}_4$ cross-relaxation produces a marked increase in the ${}^5\text{D}_3$ decay rate with increasing Tb^{3+} concentrations and introduces a non-exponential component into the initial part of the decay. The dipole–dipole interaction is found to be responsible for the cross-relaxation. The decay curves of ${}^5\text{D}_4 \rightarrow {}^7\text{F}_5$ transition exhibit an initial rise phenomenon. The two exponential fitting indicates that the initial slow rise is attributed to the ${}^5\text{D}_3 \rightarrow {}^5\text{D}_4$ cross-relaxation process.

© 2011 Elsevier B.V. All rights reserved.

1. Introduction

Recently, high quality phosphors have attracted more attention due to their practical application in the fields of display, X-ray screens, fluorescent lamps, solid state lighting, and so on [1–8]. Rare earth ions have been playing an important role in the phosphor materials due to their abundant emission colors based on their $4f\text{--}4f$ or $5d\text{--}4f$ transitions [9]. Among them, the emission spectrum of Tb^{3+} ion often shows an intense line emission near 544 nm arising from the ${}^5\text{D}_4 \rightarrow {}^7\text{F}_5$ transition [10–14]. So Tb^{3+} activated “green” phosphors are combined with Eu^{2+} activated blue phosphors and Eu^{3+} activated red phosphors to provide “trichromatic” lighting technology, a high-efficiency white light for standard illumination uses in indoor lighting [15].

Borates are good matrix for rare earth ions activated phosphors due to their low synthesis temperature, easy preparation and high luminescence efficiency [3,16–19]. The stoichiometric formula of borates $\text{MM}'_4(\text{BO}_3)_3$ (where $\text{M}=\text{Li}^+$, Na^+ or K^+ and $\text{M}'=\text{Ca}^{2+}$, Sr^{2+} or Ba^{2+}) have been reported by Wu et al. $\text{MM}'_4(\text{BO}_3)_3$ belongs to orthorhombic or cubic structure depending on the kind of cations [20,21]. Recently, these kinds of compounds attract more atten-

tion due to their potential application [3,20,21]. However, the PL properties of Tb^{3+} in these matrixes have not been reported.

In this paper, the $\text{NaBa}_4(\text{BO}_3)_3:\text{xTb}^{3+}$ phosphors have been prepared by solid-state reaction, and the PL and time-resolved luminescence properties were also investigated in detail.

2. Experimental

$\text{NaBa}_4(\text{BO}_3)_3:\text{xTb}^{3+}$ samples were prepared according to the standard solid-state technique [21]. High-purity starting materials Na_2CO_3 (Aldrich, 99.9%), BaCO_3 (Aldrich, 99.9%), H_3BO_3 (Aldrich, 99.9%), and Tb_4O_7 (Aldrich, 99.99%) were used. The well mixed materials were annealed at 700 °C for 12 h in CO weak reducing atmosphere with an intermediate grinding. Na^+ was added as a charge compensator. The structural characteristics of samples were checked by X-ray diffraction (XRD) patterns using a Philips XPert/MPD diffraction system with $\text{Cu K}\alpha$ ($\lambda=0.15405$ nm) radiation. All the samples are single phase. The PL emission and excitation spectra were measured by Fluorolog-3 Fluorescence Spectrophotometer with 450 W Xenon lamps. The luminescence decays were measured by monitoring the given emission from the samples under 266 nm pulsed laser excitation. Decay profiles were recorded by the 500 MHz digital oscilloscope (LeCroy 9350A) in which the signal was fed from PMT.

3. Results and discussion

The PL emission and excitation spectra of $\text{NaBa}_4(\text{BO}_3)_3:0.10\text{Tb}^{3+}$ phosphor are shown in Fig. 1. The sharp excitation lines at 317, 350, 370, 377, and 485 nm are observed from the excitation spectrum of the ${}^5\text{D}_4 \rightarrow {}^7\text{F}_5$ transition. These excitation lines can be ascribed to the transitions from ${}^7\text{F}_6$ to ${}^5\text{D}_j$, ${}^5\text{G}_j$, ${}^5\text{L}_{10}$, ${}^5\text{D}_3$, and ${}^5\text{D}_4$, respectively. The excitation band near 300 nm could be ascribed to the Tb^{3+} $4f^8 \rightarrow 4f^7 5d^1$ transition. In addition, $\text{NaBa}_4(\text{BO}_3)_3:\text{xTb}^{3+}$ phosphors

* Corresponding author. Tel.: +86 731 85623303; fax: +86 731 85623303.

** Corresponding author. Tel.: +82 51 629 5568; fax: +82 51 629 5549.

E-mail addresses: zhangxinminam@yahoo.com (X. Zhang), hjseo@pknu.ac.kr (H.J. Seo).

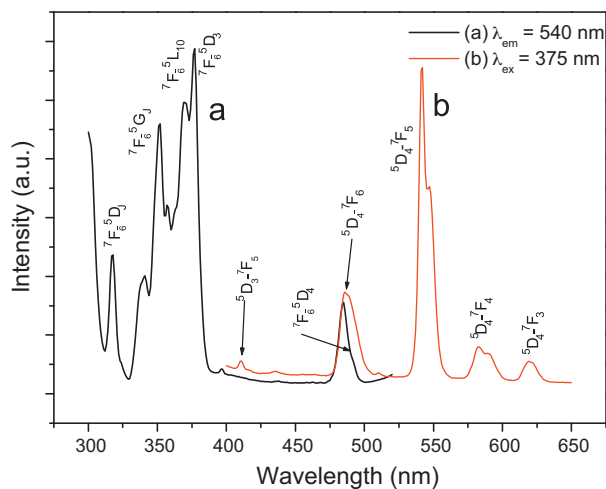


Fig. 1. PL excitation spectrum (a, $\lambda_{em}=540$ nm) and emission spectrum (b, $\lambda_{ex}=375$ nm) of $\text{NaBa}_4(\text{BO}_3)_3:0.10\text{Tb}^{3+}$ phosphor.

show intense $f \rightarrow f$ transition absorption, which may be attributed to the uneven components mix a small amount of opposite parity wave functions (e.g., $5d$) into the $4f$ wave functions; so the parity selection rule is relaxed [9]. Tb^{3+} ion with $4f^8$ configuration has complicated energy levels, so luminescence spectrum consisting of many lines due to $^5\text{D}_j \rightarrow ^7\text{F}_j$ is observed. The emission spectrum of the $\text{NaBa}_4(\text{BO}_3)_3:0.10\text{Tb}^{3+}$ sample under 375 nm UV excitation shows the $^5\text{D}_3 \rightarrow ^7\text{F}_j$ as well as the $^5\text{D}_4 \rightarrow ^7\text{F}_j$ emission lines. Among the emission lines, the $^5\text{D}_4 \rightarrow ^7\text{F}_5$ emission line at about 540 nm is the strongest one. The reason is that this transition has the largest probability for both electric-dipole and magnetic-dipole induced transitions [15]. However, the relative intensity of $^5\text{D}_3$ emission is much weaker than that of $^5\text{D}_4$ emission even in the sample with lower Tb^{3+} concentration (0.1 mol%). It is well known that the intensity ratio of the emission from $^5\text{D}_3$ to that from $^5\text{D}_4$ depends not only on the Tb^{3+} concentration [22–24], but also on the host material [15]. In borate hosts, the relative intensity of $^5\text{D}_3$ emission is much weaker than that in other hosts, such as phosphates, silicates, and aluminates [25–27], which maybe have a relation to the energy of phonons [15]. The Tb^{3+} concentration dependence on intensity of $^5\text{D}_4 \rightarrow ^7\text{F}_5$ transition has also been investigated. The intensity increases with increasing Tb^{3+} concentration, and the concentration quenching does not take place even if Tb^{3+} concentration x is equal to 10 mol% (i.e., $\text{NaBa}_4(\text{BO}_3)_3:0.10\text{Tb}^{3+}$).

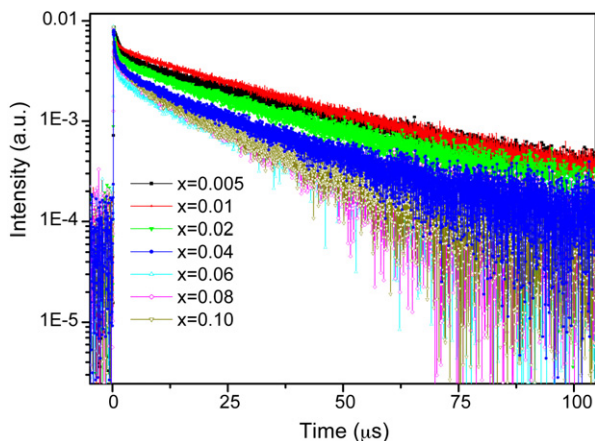


Fig. 2. Decay curves of $^5\text{D}_3 \rightarrow ^7\text{F}_5$ transition under pulsed laser excitation for $\text{NaBa}_4(\text{BO}_3)_3:x\text{Tb}^{3+}$ phosphors ($\lambda_{ex}=266$ nm, $\lambda_{em}=415$ nm).

Table 1

Parameters for Inokuti–Hirayama mechanisms for $\text{NaBa}_4(\text{BO}_3)_3:x\text{Tb}^{3+}$ ($\lambda_{ex}=266$ nm, $\lambda_{em}=415$ nm).

Concentration, x	I_0 (a.u.)	τ_0 (μs)	C/C_0
0.01	0.00716	70	0.71169
0.02	0.00569	70	0.85558
0.04	0.00495	70	1.08976
0.06	0.00412	70	1.24018
0.08	0.00516	70	1.35298
0.10	0.00520	70	1.40895

Fig. 2 depicts the decay curves of $^5\text{D}_3 \rightarrow ^7\text{F}_5$ transition of Tb^{3+} under excitation at 266 nm laser light. For the lower concentration ($x=0.005$), the decay is nearly exponential with a time constant of about 35 μs . As Tb^{3+} concentration increases, the initial part of the curves becomes non-exponential and the time constants decrease gradually ($\tau=22 \mu\text{s}$ for $x=0.10$). The possible reason could be that the $^5\text{D}_3 \rightarrow ^5\text{D}_4$ cross-relaxation produces a marked increase in the $^5\text{D}_3$ decay rate with increasing Tb^{3+} concentrations and introduces a non-exponential component into the initial part of the decay [28]. For the decay of $^5\text{D}_j \rightarrow ^7\text{F}_j$ transition, the rigorous migration effect is found in the $^5\text{D}_4 \rightarrow ^7\text{F}_5$ decay, whereas no energy migration could be found in the $^5\text{D}_3 \rightarrow ^7\text{F}_5$ decay [29]. So energy migration can be neglected. In order to determine the interactions responsible for the non-radiative relaxation from the $^5\text{D}_3$ level, the decay analysis of $^5\text{D}_3 \rightarrow ^7\text{F}_5$ transition can be carried out on employing the direct energy transfer based on the well known Inokuti–Hirayama model [30].

$$\frac{I(t)}{I_0} = \exp \left[- \left(\frac{t}{\tau_0} \right) - \left(\frac{C}{C_0} \right) \Gamma \left(1 - \frac{3}{S} \right) \left(\frac{t}{\tau_0} \right)^{\frac{3}{S}} \right] \quad (1)$$

where τ_0 is the radiative lifetime of an isolated excited Tb^{3+} ion, $\Gamma(1-3/S)$ is Euler's gamma function, C is acceptor ion concentration, C_0 is critical concentration defined as $3/(4\pi R_0^3)$ and S is the multipole interaction parameter. Many papers have reported that a dipole–dipole interaction is found to be responsible for the cross-relaxation at room temperature [28,29,31,32]. In the case of dipole–dipole interaction, the value of S is 6, and $\Gamma(1-3/S)=1.77$. The fit of the decay curves of $\text{NaBa}_4(\text{BO}_3)_3:x\text{Tb}^{3+}$ samples regarding dipole–dipole interaction indicates that the best agreement between experimental data and theoretical fits is obtained. The fitted results of $\text{NaBa}_4(\text{BO}_3)_3:x\text{Tb}^{3+}$ ($x=0.01, 0.02, 0.04, 0.06, 0.08$ and 0.10) samples are given in Table 1. The τ_0 value is about 70 μs for $^5\text{D}_3 \rightarrow ^7\text{F}_5$ transition of isolated Tb^{3+} ions in $\text{NaBa}_4(\text{BO}_3)_3:\text{Tb}^{3+}$. The critical distance for the d–d interaction is found to be about 10 Å.

The decay curves of $^5\text{D}_4 \rightarrow ^7\text{F}_5$ transition of Tb^{3+} under excitation at 266 nm pulsed laser are represented in Fig. 3. It can be seen that the decay curves show a nearly single exponential decay and does not vary obviously with increasing Tb^{3+} concentration. A single exponential fit yields a decay time 1.9 ms. The lifetimes of $^5\text{D}_4 \rightarrow ^7\text{F}_5$ transition do not change indicating that concentration quenching does not happen within the range of Tb^{3+} contents. Hao et al. has also observed similar phenomenon in $\text{CaSc}_2\text{O}_4:\text{Tb}^{3+}$ phosphor [24]. Moreover, it is noted that the decay curves of $^5\text{D}_4 \rightarrow ^7\text{F}_5$ transition exhibit an initial rise phenomenon (marked with red circle in Fig. 3). We attempted to fit these curves with double exponential equation [22,33]:

$$I(t) = I_0 \left[\exp \left(-\frac{t}{\tau_1} \right) + A \exp \left(-\frac{t}{\tau_2} \right) \right] \quad (2)$$

where I and I_0 is the luminescence intensity, t is the time, τ_1 is a decay time, τ_2 is a decay and/or rise time, A is the ratio of the two parts of the function. When $A < 0$, the second term represents rising, and for $A > 0$, the second term represents a further decay. The results of the fitting indicate that the best agreement between experimental data and theoretical fits is obtained. The result of

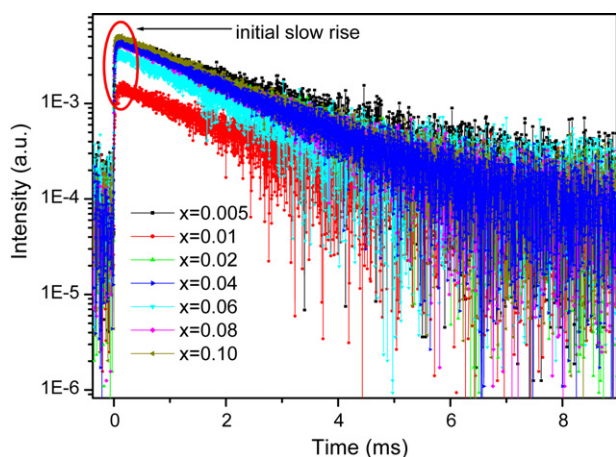


Fig. 3. Decay curves of ${}^5D_4 \rightarrow {}^7F_5$ transition under pulsed laser excitation for $\text{NaBa}_4(\text{BO}_3)_3:\text{xTb}^{3+}$ phosphors ($\lambda_{\text{ex}} = 266 \text{ nm}$, $\lambda_{\text{em}} = 544 \text{ nm}$).

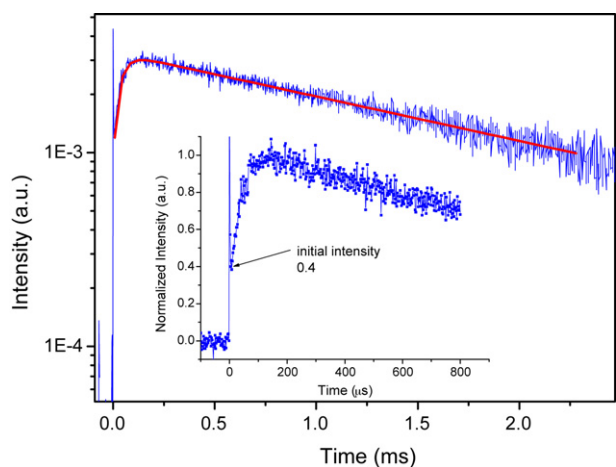


Fig. 4. Simulated decay curve of using equation (2) for $\text{NaBa}_4(\text{BO}_3)_3:0.005\text{Tb}^{3+}$ phosphor (the inset shows the initial intensity of ${}^5D_4 \rightarrow {}^7F_5$ transition).

$\text{NaBa}_4(\text{BO}_3)_3:0.005\text{Tb}^{3+}$ sample is shown in Fig. 4. The values of parameters are $\tau_1 = 1.89 \text{ ms}$ (decay time), $\tau_2 = 40 \mu\text{s}$ (rise time) and $A = -0.7833$. The initial slow rise with initial intensity (40%) of the 5D_4 emission is due to the feeding process of the 5D_4 population. It is fed about 40% of the 5D_4 population from nearby Tb^{3+} ions through the fast cross-relaxation process between Tb^{3+} (${}^5D_4 \rightarrow {}^5D_3$) and Tb^{3+} (${}^7F_6 \rightarrow {}^7F_0$) [32]. On the other hand, 60% of 5D_4 population comes directly by non-radiative relaxation process from the 5D_3 level having decay time of about $40 \mu\text{s}$ corresponding to the rise time of the 5D_4 level.

4. Conclusions

In $\text{NaBa}_4(\text{BO}_3)_3:\text{xTb}^{3+}$, the intense $f \rightarrow f$ transition absorption is observed comparing with the major Tb-doped phosphors; the

${}^5D_4 \rightarrow {}^7F_5$ transition at 540 nm is the strongest emission, and the relative intensity of 5D_3 emission is much weaker than that of 5D_4 emission even in the sample with lower Tb^{3+} concentration. The decay curves of ${}^5D_3 \rightarrow {}^7F_5$ transition can be well fitted by Inokuti–Hirayama model, and the dipole-dipole interaction is responsible for the cross-relaxation. The derived critical distance for the d–d interaction is 10 \AA . The decay curves of ${}^5D_4 \rightarrow {}^7F_5$ transition can be fitted by double exponential function, indicating that the initial slow rise with 40% of initial intensity of the 5D_4 emission is attributed to the feedings from higher energy levels and the cross-relaxation process between two Tb^{3+} ions.

Acknowledgements

This work was supported by the Science and Technology Program of Hunan Province (no. 2010FJ3092). This work was also supported by Mid-career Researcher Program through NRF grant funded by the MEST (no. 2009-0078682).

References

- [1] X.M. Zhang, W.L. Li, L. Shi, X.B. Qiao, H.J. Seo, Appl. Phys. B 99 (2010) 279–284.
- [2] X.M. Zhang, X.B. Qiao, H.J. Seo, J. Electrochem. Soc. 157 (2010) J267–J269.
- [3] X.M. Zhang, H.J. Seo, J. Alloys Compd. 503 (2010) L14–L17.
- [4] X.M. Zhang, H.J. Seo, J. Alloys Compd. 509 (2011) 2007–2010.
- [5] K. Shioi, Y. Michiue, N. Hirosaki, R.-J. Xie, T. Takeda, Y. Matsushita, M. Tanaka, Y.Q. Li, J. Alloys Compd. 509 (2011) 332–337.
- [6] H. Yokota, M. Yoshida, H. Ishibashi, T. Yano, H. Yamamoto, S. Kikkawa, J. Alloys Compd. 495 (2010) 162–166.
- [7] H. Hayashi, H. Nakano, J. Alloys Compd. 502 (2010) 360–364.
- [8] E.-J. Popovici, M. Nazarov, L. Muresan, D.Y. Noh, L.B. Tudoran, E. Bica, E. Andrea, J. Alloys Compd. 497 (2010) 201–209.
- [9] G. Blasse, B.C. Grabmaier, Luminescent Materials, Springer, Berlin, 1994.
- [10] F. Xiao, Y.N. Xue, Q.Y. Zhang, Physica B 405 (2010) 4445–4449.
- [11] X. Xiao, B. Yan, J. Am. Ceram. Soc. 93 (2010) 2195–2201.
- [12] S.S. Pitale, V. Kumar, I. Nagpure, O.M. Ntwaeaborwa, H.C. Swart, Curr. Appl. Phys. in press, doi:10.1016/j.cap.2010.08.002.
- [13] B. Lai, J. Wang, Q. Su, Appl. Phys. B 98 (2010) 41–47.
- [14] M. Gu, L. Zhu, X. Liu, S. Huang, B. Liu, C. Ni, J. Alloys Compd. 501 (2010) 371–374.
- [15] S. Shionoya, W.M. Yen, Phosphor Handbook, CRC press, New York, 1999.
- [16] X.M. Zhang, H.J. Seo, Physica B 406 (2011) 77–79.
- [17] F. Xiao, Y.N. Xue, Y.Y. Ma, Q.Y. Zhang, Physica B 405 (2010) 891–895.
- [18] R. Zhang, X. Wang, J. Alloys Compd. 509 (2011) 1197–1200.
- [19] M.A.K. Elfayoumi, M. Farouk, M.G. Brik, M.M. Elokr, J. Alloys Compd. 492 (2010) 712–716.
- [20] L. Wu, X.L. Chen, Y.P. Xu, Y.P. Sun, Inorg. Chem. 45 (2006) 3042–3047.
- [21] L. Wu, X.L. Chen, H. Li, M. He, Y.P. Xu, X.Z. Li, Inorg. Chem. 44 (2005) 6409–6414.
- [22] X.M. Zhang, J.H. Zhang, L.F. Liang, S. Qiang, Mater. Res. Bull. 40 (2005) 281–288.
- [23] Y.-C. Li, Y.-H. Chang, Y.-F. Lin, Y.-S. Chang, Y.-J. Lin, Electrochem. Solid-State Lett. 9 (2006) H74–H77.
- [24] Z. Hao, J. Zhang, X. Zhang, S. Lu, X. Wang, J. Electrochem. Soc. 156 (2009) H193–H196.
- [25] H. Zhang, Y. Wang, Y. Tao, W. Li, D. Hu, E. Feng, X. Nie, J. Electrochem. Soc. 157 (2010) J293–J296.
- [26] H. Yang, J. Shi, M. Gong, H. Liang, Mater. Lett. 64 (2010) 1034–1036.
- [27] D. Wang, N. Kodama, L. Zhao, Y. Wang, J. Electrochem. Soc. 157 (2010) J233–J237.
- [28] D.J. Robbins, B. Cockayne, B. Lent, J.L. Gasper, Solid State Commun. 20 (1976) 673–676.
- [29] N. Bodenschatz, R. Wannemacher, J. Heber, D. Mateika, J. Lumin. 47 (1990) 159–167.
- [30] M. Inokuti, F. Hirayama, J. Chem. Phys. 43 (1965) 1978–1989.
- [31] K.-S. Sohn, Y.Y. Choi, H.D. Park, Y.G. Choi, J. Electrochem. Soc. 147 (2000) 2375–2379.
- [32] A. Akrim, D. Zamboni, J.C. Coussens, J. Alloys Compd. 207–208 (1994) 99–101.
- [33] H. Kondo, T. Hirai, S. Hashimoto, J. Lumin. 108 (2004) 59–63.